Structure and Dynamics of Bis(organothiophosphoryl) Disulfides in the Solid State. X-Ray Diffraction and Cross-polarization Magic Angle Spinning Nuclear Magnetic Resonance Studies†

Paweł Knopik,[a] Lech Łuczak,[a] Marek J. Potrzebowski,*[,a] Jan Michalski,[a] Jarosław Błaszczyk[b] and Michał W. Wieczorek[b]

[a] *Center of Molecular and Macromolecular Studies, Polish Academy of Sciences, 90–362 Łódź, Sienkiewicza 112, Poland*

[b] *Technical University of Łódź, 90–924 Łódź, Stefanowskiego 4/10, Poland*

The structure and dynamics of selected bis(organothiophosphoryl) disulfides have been studied by single-crystal X-ray diffraction and high-resolution solid-state NMR spectroscopy. The crystal and molecular structures of bis[*tert*-butyl(phenyl)thiophosphoryl] disulfide **1**, bis-(diphenoxythiophosphoryl) disulfide **2** and bis[*tert*-butyl(methoxy)thiophosphoryl] disulfide **3** were determined, giving space groups of $C2/c$, $P2_12_12_1$ and $P\bar{1}$ for **1**, **2** and **3**, respectively. Both phosphorus centres of the disulfide **1** have the same absolute configuration, as have those of the disulfide **3**, although their environments were significantly different. It has been unambiguously proved that the S–S disulfide bond length varies as a function of the PSSP torsional angle. Moreover the influence the S–S–P=S conformation has on the P–S bond length is discussed. Carbon-13 NMR dipolar-dephasing experiments, using powdered samples, indicated that both the *tert*-butyl and methoxy groups attached to the phosphorus atom were in a fast regime exchange.

To date dithiophosphates have been generally considered as useful reagents in applied chemistry, in the synthesis of pesticides and oil additives and in vulcanization processes.[1–3] Owing to the large affinity of sulfur for transition metals the dithiophosphates are commonly used as ligands and several elegant applications of this class of compounds in organometallic chemistry have been reported.[4] Ongoing research by Michalski and co-workers[5,6] has also included investigations into the dithiophosphates as convenient models for mechanistic studies. Our recent work[7–9] shows that dithiophosphates with S–S linkages which mimic the cysteine CSSC skeleton possess unique static and dynamic properties in the solid state. In this paper, we report that complementary studies of bis(organothiophosphoryl) disulfides by X-ray diffraction and solid-state NMR spectroscopy can extend the knowledge about the nature of the S–S bond as well as provide general information about the molecular motion of substituents directly bonded to phosphorus. Due to the significance of the disulfide bond in natural products the physicochemical properties of the S–S linkage have been intensively studied over the last few decades. For instance, in 1966 Hordvik[10] suggested that the S–S bond length varies with the torsional angle. In the 1970s, Sugeta *et al.*[11] as well as Scheraga and co-workers[12] attempted to correlate S–S stretching frequencies with CSSC and SSCC torsional angles and the influence of 1,4-CS and 1,4-NS positions on stable conformations of aliphatic disulfides were investigated in detail.[13] Later in 1980, in order to provide a model for studies over the full range of torsional angles (0–180°) Jorgensen and Snyder[14] attempted without success to synthesize disulfides with a *trans* geometry, even when using the extremely bulky di-1-adamantyl disulfide (CSSC torsional angle 114°, *cf.* CSSC torsional angle 80–85° in an unstrained molecular environment). Hence, the relationship between the CSSC unit and its physical properties have only been obtained for torsional angles of 0–120°.[15]

Now, we report that our X-ray data for bis[*tert*-butyl-(phenyl)thiophosphoryl], bis(diphenoxythiophosphoryl)- and bis[*tert*-butyl(methoxy)thiophosphoryl] disulfides combined with literature data can be employed to establish both the changes in the S–S bond length with the PSSP torsional angle in the range 80–180° and the influence of the S–S–P=S conformation on P–S bond lengths. Furthermore, this work also shows the usefulness of ^{13}C high-resolution solid-state NMR spectroscopy in structural studies of powdered samples of dithiophosphates. In general, the NMR data obtained can provide information concerning both the content and apparent symmetry of the bis(organothiophosphoryl) disulfides and the dynamic properties of the attached substituents.

Experimental

The disulfides $[Bu^t(Ph)P(S)S]_2$ **1**, $[(PhO)_2P(S)S]_2$ **2** and $[Bu^t(MeO)P(S)S]_2$ **3** have been synthesized according to the general procedures reported elsewhere.[16]

X-Ray Crystallography.—Crystals of disulfide **1** (colourless) and **2** were grown from hexane–benzene and crystals of disulfide **3** from hexane. Intensity data were collected at room temperature using a CAD4 diffractometer in the ω–2θ scan mode, in the θ range $1 \leqslant \theta \leqslant 75°$ (**1**), $1 \leqslant \theta \leqslant 30°$ (**2**) or $1 \leqslant \theta \leqslant 28°$ (**3**), with graphite-monochromatized Cu-Kα (λ = 1.541 78 Å, **1**) or Mo-Kα (λ = 0.7107 Å, **2** and **3**) radiation. Lattice constants were refined by the least-squares fit of 25 reflections in the θ range 21.5–24.8 (**1**), 11.4–14.3 (**2**) or 5.1–13.3° (**3**). For disulfide **1** the decline in the intensities of three standard reflections (2, 4, −3; 2, 4, 3; −1, ɔ, 0) was 0.02% over 26.7 h. An absorption correction was applied using the EAC program.[17] For disulfides **2** and **3** the intensity decreases were 1.7% over 59 h (1, −6, −8; 1, −7, −6; 1, 2, −22) and 3.5%

† *Supplementary data available:* see Instructions for Authors, *J. Chem. Soc., Dalton Trans.*, 1993, Issue 1, pp. xxiii–xxviii.

over 77.9 h (−3, −1, −2; 3, 0, −2; 0, −3, 1), respectively. The structures were solved by direct methods and refined by full-matrix least squares using *F*. Hydrogen atoms were placed geometrically at idealized positions (**1**) or found from Fourier-difference maps (**2** and **3**) and set as riding with fixed isotropic thermal parameters, $U(H) = 1.3$ (**1**) or 4.00 (**2** and **3**) $U_{eq}(C)$.

All calculations were performed with the Enraf-Nonius SDP crystallographic computing package,[17a] excluding the structure solving by direct methods which used the SHELXS 86 program.[18] Scattering factors were taken from ref. 19. A summary of the crystal data and the experimental details is given in Table 1.

Additional material available from the Cambridge Crystallographic Data Centre comprises H-atom coordinates, thermal parameters and remaining bond lengths and angles.

Solid-state NMR Measurements.—Cross-polarization magic angle spinning (CP MAS) solid-state ^{13}C and ^{31}P NMR spectra were recorded on a Bruker 300 MSL instrument with high power proton decoupling at 75.468 MHz for ^{13}C and 121.496 MHz for ^{31}P. Powder samples of the bis(organothiophosphoryl) disulfides were placed in a cylindrical rotor and spun at 2.5–5.0 kHz. For the ^{13}C NMR experiments, the field strength for the ^{1}H decoupling was 1.05 mT; a contact time of 1–5 ms, a repetition time of 6 s (with the exception of **2**) and a spectral width of 20 kHz were used, and the free induction decay (FID) was represented by 8K data points. Spectra were accumulated 100–500 times to achieve a reasonable signal-to-noise ratio. The ^{13}C chemical shifts were calibrated indirectly through the glycine carbonyl peak observed at δ 176.34 relative to tetramethysilane. For the ^{31}P NMR experiments, the field strength for the ^{1}H decoupling was 1.05 mT; a contact time of 5 ms, a repetition time of 6 s and spectral width of 50 kHz were used and 8K data points represented the FID. Spectra were accumulated 12–100 times, which gave a reasonable signal-to-noise ratio. The ^{31}P chemical shifts were calibrated indirectly through the 85% phosphoric acid peak set at δ 0.

Results and Discussion

Structural Studies.—The thermal ellipsoidal plot and numbering scheme of bis[*tert*-butyl(phenyl)thiophosphoryl] disulfide **1** is shown in Fig. 1 and the atomic coordinates are in Table 2. Compound **1** crystallized in the space group *C*2/*c*, with a unit cell consisting of four molecules (half of the molecule is an asymmetric unit). The *tert*-butyl(phenyl)thiophosphoryl groups with the same absolute configuration at the phosphorus centres are bridged by a disulfide unit. The *C*2/*c* is a centrosymmetric space group hence the unit cell consists of pairs of molecules with opposite absolute configuration. In consequence compound **1** can be considered as a racemic mixture of *R*,*R*- and *S*,*S*-disulfides.[20] The bond lengths and angles (Table 3) calculated for both the *tert*-butyl and phenyl groups are typical and do not differ considerably from the ideal values. The S–S bond length was found to be 2.031(2) Å and is significantly

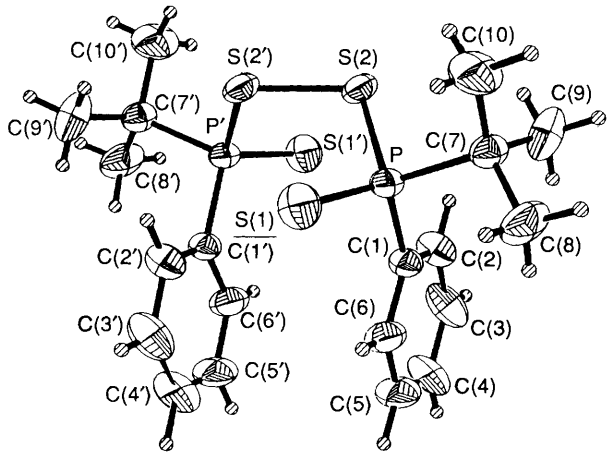

Fig. 1 Molecular structure of disulfide **1** with the atomic numbering system

Table 1 Crystal data and experimental details

Formula	$C_{20}H_{28}P_2S_4$	$C_{24}H_{20}O_4P_2S_4$	$C_{10}H_{24}O_2P_2S_4$
M	458	562	366.5
Crystal symmetry	Monoclinic	Orthorhombic	Triclinic
Crystal dimensions/mm	0.15 × 0.3 × 0.6	0.2 × 0.3 × 0.5	0.15 × 0.4 × 0.5
Space group	*C*2/*c*	$P2_12_12_1$	$P\bar{1}$
a/Å	20.035(2)	6.629(2)	7.916(3)
b/Å	9.231(2)	11.584(1)	10.501(5)
c/Å	12.978(2)	34.536(5)	12.461(4)
α/°	—	—	110.11(3)
β/°	102.30(1)	—	98.77(3)
γ/°	—	—	99.96(3)
U/Å^3	2344(5)	2651.9(8)	932(16)
Z	4	4	2
μ/cm^{-1}	50.1	4.9	6.5
D_c/g cm^{-3}	1.299(2)	1.409(2)	1.305(3)
F(000)	484	1160	388
$2\theta_{max}$/°	150	60	56
Scan width/°	0.80 + 0.14 tan θ	0.80 + 0.35 tan θ	1.40 + 0.35 tan θ
h,*k*,*l* Ranges	0–25, 0–11, −16 to 16	0–9, 0–16, 0–48	0–10, −13 to 13, −16 to 16
Total no. of reflections measured	2643	4389	4809
No. observed [$I \geqslant 3\sigma(I)$]	2406	2897	1080
No. refined	118	307	163
Maximum shift/error	0.01	0.02	0.01
Maximum residual peak in final difference map/e Å^{-3}	0.241	—	0.798
EAC correction:			
minimum	0.7875	0.9740	0.8123
maximum	0.9975	0.9991	0.9999
average	0.9244	0.9904	0.9000
R (*w* = 1)	0.050	0.036	0.083

Table 2 Atomic coordinates for **1**

Atom	*x*	*y*	*z*	Atom	*x*	*y*	*z*
S(1)	0.581 68(6)	0.900 7(1)	0.963 98(8)	C(5)	0.587 6(3)	0.490 4(5)	0.752 4(5)
S(2)	0.544 57(5)	1.074 1(1)	0.724 62(8)	C(6)	0.596 4(2)	0.620 1(5)	0.808 7(4)
P	0.605 39(5)	0.918 5(1)	0.827 41(7)	C(7)	0.692 7(2)	0.988 1(4)	0.831 1(3)
C(1)	0.595 1(2)	0.749 7(4)	0.752 8(3)	C(8)	0.742 3(2)	0.879 3(6)	0.896 1(4)
C(2)	0.585 1(2)	0.747 8(5)	0.643 4(3)	C(9)	0.706 7(2)	1.003 5(6)	0.720 4(4)
C(3)	0.576 6(3)	0.616 6(6)	0.589 2(4)	C(10)	0.700 4(3)	1.135 3(5)	0.889 3(5)
C(4)	0.578 6(3)	0.487 5(5)	0.645 3(5)				

Table 3 Bond lengths (Å) and angles (°) for **1**

S(1)–P	1.938(2)	C(1)–C(2)	1.392(6)	C(4)–C(5)	1.363(9)	C(7)–C(9)	1.529(7)
S(2)–P	2.153(1)	C(1)–C(6)	1.396(6)	C(5)–C(6)	1.394(7)	C(7)–C(10)	1.546(7)
P–C(1)	1.823(4)	C(2)–C(3)	1.393(7)	C(7)–C(8)	1.532(6)	S(2')–S(2)	2.031(2)
P–C(7)	1.855(5)	C(3)–C(4)	1.393(8)				
S(1)–P–S(2)	114.01(7)	C(1)–P–C(7)	108.0(2)	C(2)–C(3)–C(4)	119.5(5)	P–C(7)–C(9)	111.6(3)
S(1)–P–C(1)	113.0(1)	P–C(1)–C(2)	121.9(4)	C(3)–C(4)–C(5)	120.0(5)	P–C(7)–C(10)	108.3(3)
S(1)–P–C(7)	114.8(1)	P–C(1)–C(6)	118.0(3)	C(4)–C(5)–C(6)	121.7(5)	C(8)–C(7)–C(9)	110.6(4)
S(2)–P–C(1)	104.9(1)	C(2)–C(1)–C(6)	120.1(4)	C(1)–C(6)–C(5)	118.6(5)	C(8)–C(7)–C(10)	108.8(3)
S(2)–P–C(7)	101.0(1)	C(1)–C(2)–C(3)	120.1(4)	P–C(7)–C(8)	106.5(3)	C(9)–C(7)–C(10)	111.0(5)

The primed atom is from the symmetrical $(1 - x, y, \frac{3}{2} - z)$ moiety.

shorter than those seen for other bis(organothiophosphoryl) disulfides reported elsewhere,[8,21–23] whereas the P–S bond length [2.153(1) Å] in the PSSP unit of the disulfude **1** is much longer (*cf. ca.* 2.009 Å). The S–P=S angle was 114.01(7)°

The thermal ellipsoidal plot of bis(diphenoxythiophosphoryl) disulfide **2** is shown in Fig. 2 and the atomic coordinates are in Table 4. Compound **2** crystallized in the space group $P2_12_12_1$. The unit cell consists of four molecules (one molecule is an independent unit). Consistent with a previous report on disulfides,[8] a relationship between the PSSP torsional angle [112.04(6)°] and the S–S bond length [2.072(1) Å] was observed (Table 5). The phosphorus thiono and thiolo bond lengths were 1.900(2) and 2.080(1) Å, respectively, and the S–P=S angle was 107.69(7)°. The diphenoxythiophosphoryl moieties with opposed terminal sulfur atoms S(3) and S(4) are bridged by a disulfide unit. Bond lengths and angles of the phenoxy groups do not differ considerably from typical values.

The thermal ellipsoidal plot of bis[*tert*-butyl(methoxy)thiophosphoryl] disulfide **3** is shown in Fig. 3 and the atomic coordinates are in Table 6. The disulfide **3** crystallized in the space group $P\bar{1}$ and the unit cell consists of two molecules with one molecule as an independent unit. Careful inspection of the molecular structure in terms of the stereochemistry at the phosphorus atoms shows that both centres have the same absolute configuration. As in case of the disulfide **1** the unit cell consists of *R,R*- and *S,S*-disulfides. Surprisingly, the geometrical parameters for the P(1) and P(2) environments were found to be dramatically different. As seen in Table 7 the P(1)–S(1) bond was 2.093(8) Å whereas the P(2)–S(2) bond [2.139(6) Å] is significantly longer (*ca.* 0.04 Å). Analysis of the P=S bond lengths shows that P(1)=S(3) and P(2)=S(4) are comparable, 1.923(7) and 1.913(8) Å. The S=P–S angles are, however, significantly different [S(1)–P(1)=S(3) 101.2(3) and S(2)–P(2)=S(4) 115.3(3)°]. The S–S disulfide bond length is 2.048(9) Å for a PSSP torsional angle of 103.7(3)°. The values of the calculated bond lengths and angles for the *tert*-butyl and methoxy groups do not differ significantly from the typical ones.

The results presented here combined with our previous data[8] enable us to form general conclusions regarding the relationship between the disulfide bond length and the PSSP torsional angle. Our results are compared with X-ray diffraction data of thiophosphoryl disulfides[21,23–25] and the most significant geometrical parameters employed in the discussion below are collected in Table 8.

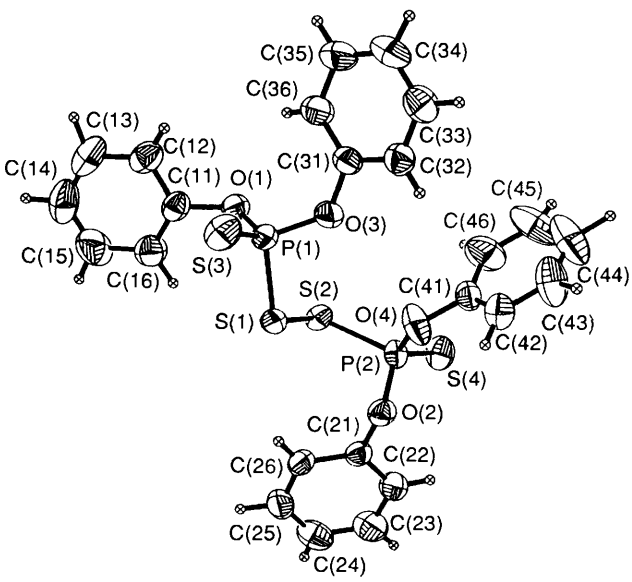

Fig. 2 Molecular structure of disulfide **2** with the atomic numbering system

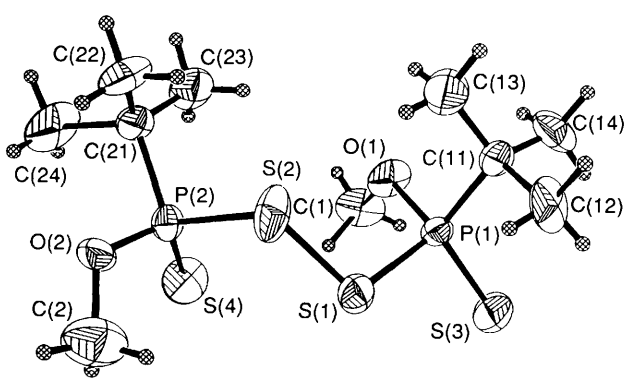

Fig. 3 Molecular structure of disulfide **3** with the atomic numbering system

As suggested previously,[8] the changes in the disulfide bond length in the PSSP skeleton *versus* the torsional angle closely follow the geometrical changes in the CSSC unit. Fig. 4 displays

Table 4 Atomic coordinates for **2**

Atom	*x*	*y*	*z*	Atom	*x*	*y*	*z*
S(1)	0.108 4(2)	0.303 80(8)	0.110 02(3)	C(22)	0.597 1(7)	0.561 2(4)	0.022 2(1)
S(2)	0.007 4(2)	0.423 02(9)	0.069 73(3)	C(23)	0.694 6(8)	0.523 3(4)	−0.010 7(1)
S(3)	−0.049 2(2)	0.184 7(1)	0.188 45(4)	C(24)	0.701 5(8)	0.407 9(4)	−0.019 5(1)
S(4)	0.121 6(2)	0.686 2(1)	0.048 12(4)	C(25)	0.612 9(7)	0.329 0(4)	0.004 4(1)
P(1)	−0.132 6(2)	0.285 23(9)	0.148 05(3)	C(26)	0.515 2(6)	0.365 0(3)	0.037 9(1)
P(2)	0.192 2(2)	0.563 41(8)	0.082 03(3)	C(31)	−0.318 2(7)	0.443 5(3)	0.189 7(1)
O(1)	−0.323 6(4)	0.247 4(2)	0.123 24(8)	C(32)	−0.245 9(8)	0.525 6(4)	0.214 7(1)
O(2)	0.417 6(4)	0.516 2(2)	0.080 67(8)	C(33)	−0.367 6(8)	0.559 8(4)	0.245 0(1)
O(3)	−0.192 6(5)	0.413 3(2)	0.157 90(8)	C(34)	−0.556 5(8)	0.511 7(5)	0.250 1(1)
O(4)	0.179 4(6)	0.579 5(3)	0.127 24(8)	C(35)	−0.625 4(8)	0.429 6(5)	0.224 9(2)
C(11)	−0.364 0(7)	0.131 7(3)	0.112 3(1)	C(36)	−0.508 1(7)	0.395 8(4)	0.193 9(1)
C(12)	−0.518 1(8)	0.074 7(4)	0.130 6(1)	C(41)	0.124 5(7)	0.675 5(3)	0.148 6(1)
C(13)	−0.564 5(9)	−0.036 7(4)	0.117 7(2)	C(42)	0.255 2(8)	0.704 9(4)	0.177 9(1)
C(14)	−0.460 9(9)	−0.087 4(5)	0.089 1(2)	C(43)	0.206(1)	0.793 9(4)	0.202 1(2)
C(15)	−0.308(1)	−0.029 1(5)	0.071 4(2)	C(44)	0.031(1)	0.851 1(5)	0.197 0(2)
C(16)	−0.259 2(8)	0.083 7(4)	0.082 2(2)	C(45)	−0.098(1)	0.822 6(6)	0.168 8(2)
C(21)	0.507 3(6)	0.481 3(3)	0.045 7(1)	C(46)	−0.053 9(9)	0.731 2(5)	0.143 6(2)

Table 5 Bond lengths (Å) and angles (°) for **2**

S(1)–S(2)	2.072(1)	O(2)–C(21)	1.404(5)	C(21)–C(22)	1.368(6)	C(33)–C(34)	1.381(8)
S(1)–P(1)	2.079(2)	O(3)–C(31)	1.422(5)	C(21)–C(26)	1.376(5)	C(34)–C(35)	1.368(7)
S(2)–P(2)	2.080(1)	O(4)–C(41)	1.385(5)	C(22)–C(23)	1.381(7)	C(35)–C(36)	1.379(7)
S(3)–P(1)	1.900(2)	C(11)–C(12)	1.371(6)	C(23)–C(24)	1.371(8)	C(41)–C(42)	1.375(6)
S(4)–P(2)	1.901(2)	C(11)–C(16)	1.370(7)	C(24)–C(25)	1.364(7)	C(41)–C(46)	1.358(7)
P(1)–O(1)	1.591(4)	C(12)–C(13)	1.399(7)	C(25)–C(26)	1.391(6)	C(42)–C(43)	1.366(7)
P(1)–O(3)	1.573(3)	C(13)–C(14)	1.339(8)	C(31)–C(32)	1.371(6)	C(43)–C(44)	1.35(2)
P(2)–O(2)	1.591(4)	C(14)–C(15)	1.364(9)	C(31)–C(36)	1.382(6)	C(44)–C(45)	1.34(1)
P(2)–O(4)	1.575(3)	C(15)–C(16)	1.397(8)	C(32)–C(33)	1.380(7)	C(45)–C(46)	1.402(8)
O(1)–C(11)	1.417(5)						
S(2)–S(1)–P(1)	104.18(7)	O(2)–P(2)–O(4)	96.9(2)	O(2)–C(21)–C(22)	120.0(3)	C(32)–C(33)–C(34)	120.7(5)
S(1)–S(2)–P(2)	101.18(6)	P(1)–O(1)–C(11)	123.7(3)	O(2)–C(21)–C(26)	117.8(3)	C(33)–C(34)–C(35)	120.1(5)
S(1)–P(1)–S(3)	107.69(7)	P(2)–O(2)–C(21)	121.4(3)	C(22)–C(21)–C(26)	122.0(4)	C(34)–C(35)–C(36)	120.2(5)
S(1)–P(1)–O(1)	107.4(1)	P(1)–O(3)–C(31)	123.2(3)	C(21)–C(22)–C(23)	118.5(5)	C(31)–C(36)–C(35)	118.8(4)
S(1)–P(1)–O(3)	103.6(1)	P(2)–O(4)–C(41)	129.7(3)	C(22)–C(23)–C(24)	120.5(5)	O(4)–C(41)–C(42)	115.3(4)
S(3)–P(1)–O(1)	117.3(1)	O(1)–C(11)–C(12)	118.3(4)	C(23)–C(24)–C(25)	120.4(5)	O(4)–C(41)–C(46)	122.9(4)
S(3)–P(1)–O(3)	119.5(1)	O(1)–C(11)–C(16)	119.4(4)	C(24)–C(25)–C(26)	120.2(4)	C(42)–C(41)–C(46)	121.8(4)
O(1)–P(1)–O(3)	100.1(2)	C(12)–C(11)–C(16)	122.2(4)	C(21)–C(26)–C(25)	118.3(4)	C(41)–C(42)–C(43)	119.2(5)
S(2)–P(2)–S(4)	108.31(8)	C(11)–C(12)–C(13)	117.5(4)	O(3)–C(31)–C(32)	116.9(4)	C(42)–C(43)–C(44)	119.6(6)
S(2)–P(2)–O(2)	106.2(1)	C(12)–C(13)–C(14)	121.8(6)	O(3)–C(31)–C(36)	121.1(4)	C(43)–C(44)–C(45)	121.8(6)
S(2)–P(2)–O(4)	105.2(1)	C(13)–C(14)–C(15)	119.7(5)	C(32)–C(31)–C(36)	122.0(5)	C(44)–C(45)–C(46)	120.3(6)
S(4)–P(2)–O(2)	118.0(1)	C(14)–C(15)–C(16)	121.1(5)	C(31)–C(32)–C(33)	118.2(5)	C(41)–C(46)–C(45)	117.4(6)
S(4)–P(2)–O(4)	120.6(1)	C(11)–C(16)–C(15)	117.7(5)				

Table 6 Atomic coordinates for **3**

Atom	*x*	*y*	*z*	Atom	*x*	*y*	*z*
S(1)	0.1430(7)	0.5372(4)	0.6511(4)	C(2)	0.338(3)	0.819(2)	0.488(2)
S(2)	0.3888(7)	0.5812(5)	0.6199(5)	C(11)	0.254(3)	0.326(2)	0.776(1)
S(3)	−0.0790(7)	0.4585(5)	0.8141(5)	C(12)	0.134(3)	0.203(2)	0.660(2)
S(4)	0.3306(8)	0.9040(5)	0.7736(6)	C(13)	0.441(2)	0.352(2)	0.762(2)
P(1)	0.1597(6)	0.4778(4)	0.7957(4)	C(14)	0.234(3)	0.289(2)	0.881(1)
P(2)	0.4753(7)	0.8040(4)	0.6843(4)	C(21)	0.706(2)	0.834(2)	0.747(2)
O(1)	0.310(2)	0.595(1)	0.903(1)	C(22)	0.796(2)	0.745(2)	0.668(2)
O(2)	0.492(2)	0.829(1)	0.569(1)	C(23)	0.719(3)	0.820(2)	0.866(2)
C(1)	0.266(3)	0.719(2)	0.977(2)	C(24)	0.795(3)	0.989(2)	0.768(2)

the experimental (upper) curve for the PSSP unit and the theoretical (lower) curve of the CSSC backbone taken from the work of Aida and Nagata.[24] As stated in the Introduction, due to the lack of suitable models, the relationship between the S–S bond lengths and the CSSC unit in the range 115–180° has never been confirmed by experimental data. It can be concluded that in the region 110–180° the fit of the PSSP curve follows the data for the CSSC skeleton, however, the S–S distances for the former are slightly greater. In the region about 90° the disulfide linkage is significantly shorter than those for the carbon analogues. Another unique feature of the S=PSSP=S unit is the large difference in the P–S distances which varied from 2.079(2) (disulfide **2**) to 2.153(1) Å (disulfide **1**). These differences can be explained in terms of the changes in the S–S–P=S conformation. The bis(diaryloxy- and bis(dialkoxy-thiophosphoryl) disulfides contain a planar zigzag array of linkages, the S–S–P=S units having an *anti-anti* geometry. These structures are characterized by short (*ca.* 2.085 Å) P–S bonds. The distortion from an *anti* geometry as in the case of bis[(−)menthyloxy(phenyl)thiophosphoryl] disulfide causes a P–S bond elongation (2.10 Å,

Table 7 Bond lengths (Å) and angles (°) for **3**

S(1)–S(2)	2.048(9)	P(1)–O(1)	1.62(2)	O(1)–C(1)	1.45(2)	C(11)–C(14)	1.51(3)
S(1)–P(1)	2.093(8)	P(1)–C(11)	1.84(2)	O(2)–C(2)	1.42(3)	C(21)–C(22)	1.47(3)
S(2)–P(2)	2.139(6)	P(2)–O(2)	1.57(1)	C(11)–C(12)	1.59(3)	C(21)–C(23)	1.53(3)
S(3)–P(1)	1.923(7)	P(2)–C(21)	1.80(2)	C(11)–C(13)	1.51(3)	C(21)–C(24)	1.56(3)
S(4)–P(2)	1.913(8)						
S(2)–S(1)–P(1)	109.4(3)	O(1)–P(1)–C(11)	99.8(7)	P(1)–O(1)–C(1)	119(1)	C(13)–C(11)–C(14)	114(2)
S(1)–S(2)–P(2)	106.5(4)	S(2)–P(2)–S(4)	115.3(3)	P(2)–O(2)–C(2)	121(1)	P(2)–C(21)–C(22)	113(2)
S(1)–P(1)–S(3)	101.2(3)	S(2)–P(2)–O(2)	101.7(4)	P(1)–C(11)–C(12)	106(1)	P(2)–C(21)–C(23)	107(1)
S(1)–P(1)–O(1)	108.4(7)	S(2)–P(2)–C(21)	102.4(6)	P(1)–C(11)–C(13)	113(1)	P(2)–C(21)–C(24)	107(1)
S(1)–P(1)–C(11)	113.1(7)	S(4)–P(2)–O(2)	115.7(7)	P(1)–C(11)–C(14)	105(1)	C(22)–C(21)–C(23)	115(2)
S(3)–P(1)–O(1)	117.1(6)	S(4)–P(2)–C(21)	120.3(6)	C(12)–C(11)–C(13)	109(2)	C(22)–C(21)–C(24)	107(2)
S(3)–P(1)–C(11)	117.5(7)	O(2)–P(2)–C(21)	89.6(9)	C(12)–C(11)–C(14)	110(1)	C(23)–C(21)–C(24)	109(2)

Table 8 Geometrical parameters for the disulfides

Disulfide	S–S/Å	S=P–S/°	PSSP/°	P–S/Å	S=P–S–S/°	P=S/Å	Ref.
$[(Pr^iO)_2P(S)S]_2$	2.115	104.8	180.0	2.085	180.0	1.920	22
$[(CMe_3CH_2O)_2P(S)S]_2$	2.127	106.6	180.0	2.088	180.0	1.911	8
$[Ph(RO)P(S)S]_2$ [R = L(−)-menthyl]	2.075	103.8	113.7	2.101	159.6	1.926	21
2 $[(PhO)_2P(S)S]_2$	2.072	107.7	112.0	2.079	176.2	1.900	This
		108.3		2.080	179.3	1.901	work
$[(MeO)_2P(S)S]_2$	2.069	105.4	105.7	2.088	180.0	1.904	8
3 $[Bu^t(MeO)P(S)S]_2$	2.048	101.2	103.7	2.093	175.4	1.923	This
		115.3		2.139	9.5	1.913	work
1 $[Bu^t(Ph)P(S)S]_2$	2.031	114.0	93.7	2.153	27.6	1.938	This work
$[\overline{OCH_2CMe_2CH_2OP(S)S}]_2$	2.036	116.0	89.7	2.112	−81.5	1.894	23
				2.118	46.4	1.891	

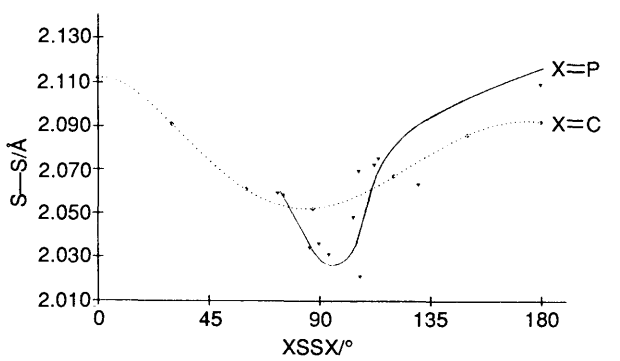

Fig. 4 Changes in the S–S bond length *versus* the CSSC and PSSP torsional angles; (· · · ·) theoretical[24] curve for the CSSC unit; (——) experimental curve for the PSSP unit

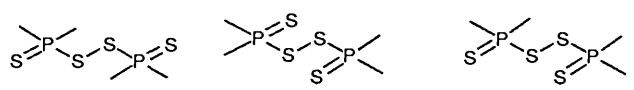

anti-anti *syn-syn* *anti-syn*

S–S–P=S 159.6°).[21] Bis(5,5-dimethyl-2-thiono-1,3,2λ^5-dioxaphosphorin-2-yl) disulfide can also be included in this group (Table 8).

The *syn-syn* conformation of the zigzag array is exhibited by the disulfide **1** with an S–S–P=S torsional angle of 27.6(2)° and the longest P–S bond 2.153(1) Å.

The most spectacular case which unambiguously answers the question of the influence of the S–S–P=S conformation on the P–S bond length was found for the disulfide **3**. The structure consists of two *tert*-butyl(methoxy)thiophosphoryl groups, with the same absolute configuration at the phosphorus centres, bridged by a disulfide linkage. The S=PSSP=S backbone possesses features common to both the *anti-anti* and *syn-syn* conformations [S–S–P=S 175.4(3) and 9.5(5)°], hence this disulfide can be termed the *anti-syn* conformation. The influence of conformation changes on the P–S bond lengths is apparent. For an *anti* conformation the P–S distance was 2.093(8) Å whereas for the *syn* conformation it was significantly longer [2.139(6) Å]. Our results are consistent with recent data of Burunda *et al.*[25] who found a similar geometrical relationship for bis(dicyclohexylthiophosphoryl) disulfide. As in our case of *anti-syn* geometry the differences in the P–S bond lengths and the S–P=S angles were found to be 0.04 Å and 10°, respectively. Hence, it can be unambiguously concluded that the relationship between the S–S–P=S unit and its geometrical parameters is general. However, it seems that the explanation of these changes based on the overlapping effect of a filled non-bonding p orbital on the bridging sulfur atom with the d_{xz} and d_{yz} orbitals on the phosphorus atom does not cover all the geometrical details. Furthermore, careful inspection of the anisotropic thermal parameters (deposited) suggests that some substituents attached to the phosphorus undergo dynamic processes in the solid. As seen in Fig. 5, the ellipsoids which correspond to the *tert*-butyl methyl carbons in disulfides **1** and **3** are large. Their shape suggests a fast rotation of the methyl groups around a C_3 axis.

Solid-state NMR Studies.—In order to study in detail the dynamics of the substituents bonded to phosphorus additional results were gained from high-resolution solid-state NMR spectroscopy. In particular, the CP MAS technique was considered as the method of choice because this type of experiment can provide information on the dynamics (for instance *via* dipolar dephasing or measurements of the relaxation parameters) as well as on the content and apparent symmetry of the unit cell.[26]

Fig. 6 displays the ^{13}C NMR spectra of the three disulfides recorded at room temperature. All the spectra show well resolved resonances which can be assigned to individual alkyl and aryl groups. For the disulfide **1** [Fig. 6(*a*)], the six aromatic signals of the phenyl ring in the region δ 130–140 and the single resonance line of the quaternary carbon of the *tert*-butyl group

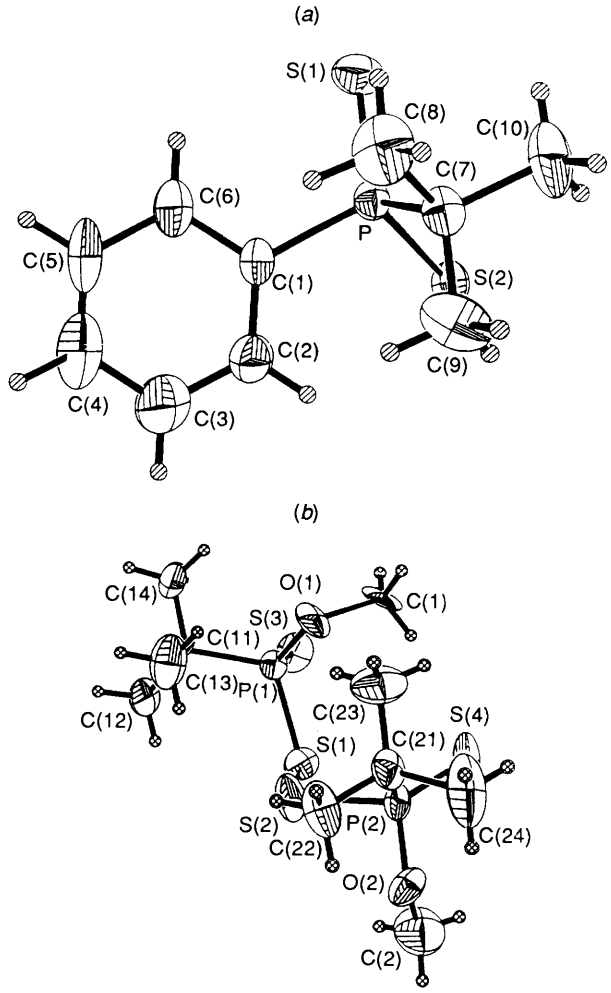

Fig. 5 Molecular structure of disulfides **1** (*a*) and **3** (*b*), each viewed along the P–C bond of the *tert*-butyl group

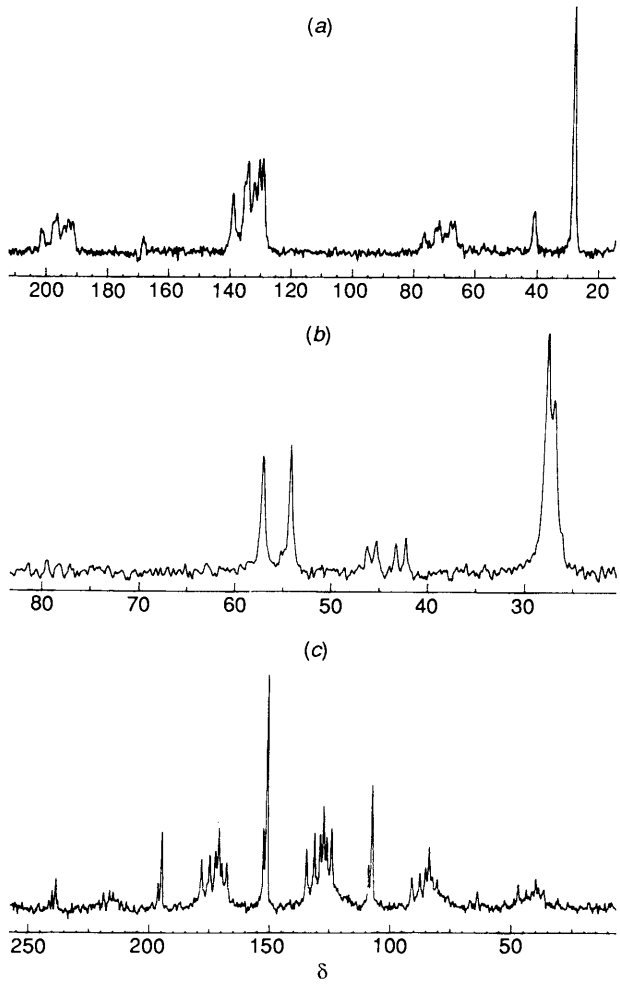

Fig. 6 Solid-state 75.46 MHz ^{13}C CP MAS NMR spectra (with 5 Hz line broadening) of the disulfides **1** (*a*), **3** (*b*) and **2** (*c*). The aromatic signals are in the regions δ 130–140 and 124–152 for disulfides **1** and **3** respectively. The residual peaks, with the exception of those at δ 27.97 and 40.86 for **1**, are the spinning sidebands (see text)

(δ 40.86) suggest that the half molecule of **1** is an asymmetric unit. This result is consistent with the X-ray data (the unit cell of the disulfide **1** is shown in Fig. 7). The observed sharp, single line instead of the expected three resonances for the crystallographically non-equivalent *tert*-butyl methyl groups (δ 27.97) can be explained by the overlapping effect and the fast reorientation of the *tert*-butyl group in the solid.

These same effects are seen [Fig. 6(*b*)] for the *tert*-butyl methyl groups of the disulfide **3**, however, in this case two resonances at δ 27.89 and 27.08 can be unambiguously assigned. Furthermore, two sharp signals at δ 57.16 and 54.34 for the methoxy carbons provide evidence that one molecule of the disulfide **3** is an independent unit. The unexpected presence of four quaternary carbon signals (δ 46.41, 45.36, 43.33 and 42.28) can be slightly misleading, however, the analysis of the X-ray data clearly shows that the unit cell (displayed in Fig. 8) consists of two molecules with presumably magnetically non-equivalent quaternary carbons.

The spectrum of the disulfide **2** shown in Fig. 6(*c*) was obtained with a 60 s delay instead of the usual 6 s because of a poor signal-to-noise ratio when standard parameters were used. This indicates that the disulfide **2** has a relatively long T_1(H), but why it is so much longer compared to other disulfides is not perfectly clear. However, as shown by Brown,[27] even very small variations in the structures can cause large variations in T_1(H). The spectrum shows well resolved signals for each individual aromatic carbon atom in the region δ 124–152. These resonances, owing to the large chemical shift anisotropy typical for phenyl rings [also seen in Fig. 6(*a*)], are symmetrically

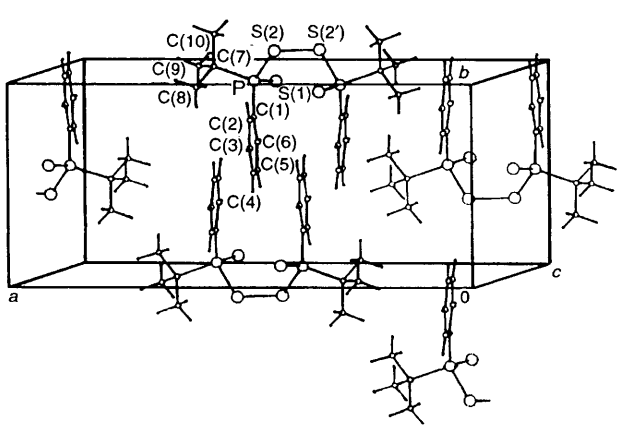

Fig. 7 Molecular packing in the unit cell of the disulfide **1**

flanked by the spinning sidebands. As one can see, the most downfield resonances of the quaternary O–C carbons can be considered as a useful tool in studying the content and symmetry of the unit cell. The two signals at δ 152.53 and 151.14 (with roughly calculated intensity 1:3) instead of the expected four lines suggest that one molecule is an independent unit. The distorted intensity of the quaternary signals may be the result of the magnetic equivalence of three out of the four crystallographically non-equivalent carbon atoms. The unit cell of the disulfide **2** is shown in Fig. 9.

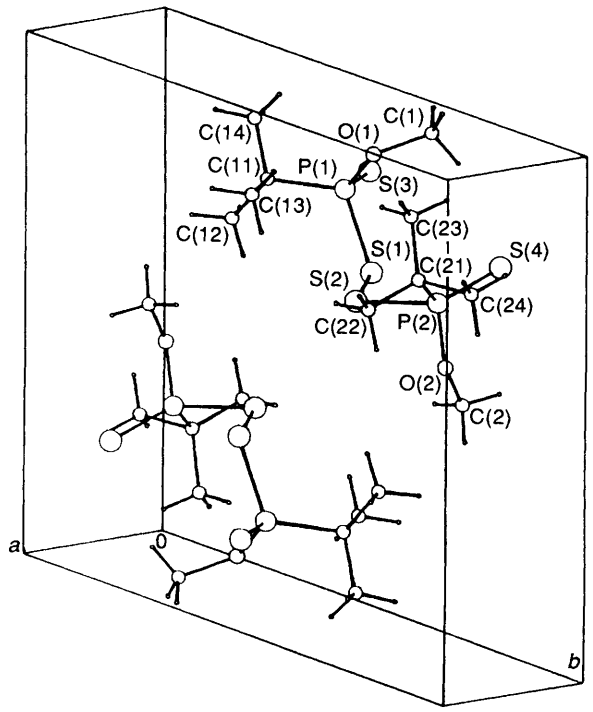

Fig. 8 Molecular packing in the unit cell of the disulfide **3**

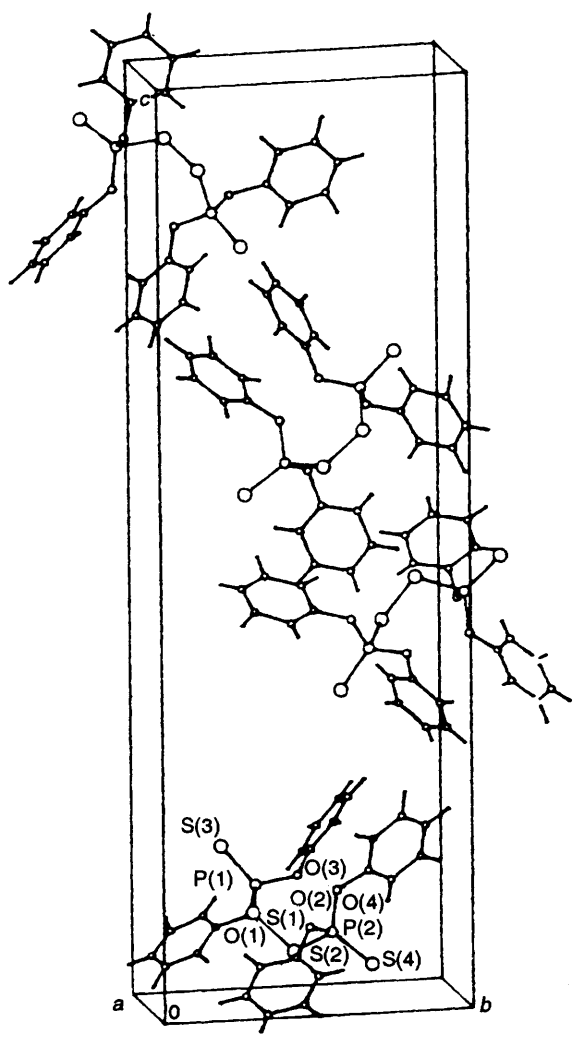

Fig. 9 Molecular packing in the unit cell of the disulfide **2**

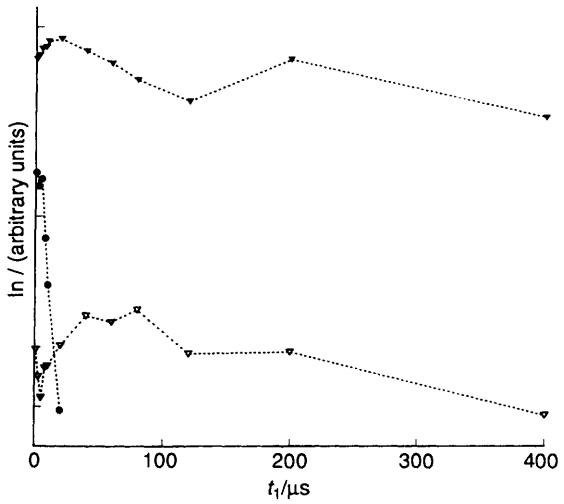

Fig. 10 Plot of ln*I versus* t_1 for the *tert*-butyl methyl group (▼), the quaternary carbon (▽) and the aromatic carbon (●) of the disulfide **1**

The preliminary results regarding the dynamics of bis(organothiophosphoryl) disulfides in the solid state were taken from dipolar-dephasing experiments. Dipolar-dephasing and conventional cross-polarization experiments can provide significant, complementary information about freedom of motion.[28,29] In our investigations we have employed the commonly used sequence, where a variable interruption time t_1 in the proton spin decoupling is inserted at the end of the cross-polarization period and before the data acquisition.[30] During this time, the carbon magnetization is influenced by the heteronuclear dipole interaction. As shown in the theoretical model of Demco *et al.*[31] the carbon atoms polarize according to the following relative rates CH_3(static) > CH_2 > CH= CH_3(rotated) > C(non-protonated). Hence, in the dipolar-dephasing experiment the rates of signal decay have to obey this same relationship. Opella and Frey[32] have shown that for a dephasing time of 40 μs the resonances of the methine and methylene carbons are greatly attenuated. Thus, in order to obtain a spectrum containing only signals of rotating methyls and quaternary carbons a dephasing period of 40–120 μs should be sufficient.

A plot of the signal intensities (*I*) *vs.* the dipolar-dephasing delay t_1 for the disulfide **1** is shown in Fig. 10. As predicted, the resonance of the *tert*-butyl quaternary carbon decayed very slowly and after t_1 = 400 μs the signal could still be recorded. In contrast, the resonances of the aromatic ring (for clarity only the most upfield signal is shown) disappear at t_1 = 40 μs. The *tert*-butyl methyl groups revealed features characteristic of rapidly rotating substituents. For a dipolar-dephasing time over 400 μs the methyl signals show an almost unchanged intensity.

These studies also show that the overall loss of signal intensity in the dipolar-dephasing experiment is a complex phenomenon. The carbon signal can decay as a multiple exponential depending on the proximity of the protons, the molecular motion and the extent of signal overlap. The decay can also be complicated by oscillatory changes in the signal intensities arising from dipolar and rotational modulations superimposed on the exponential decays. The dipolar modulations for some carbons are usually observed as damped oscillations in signal intensity before the first rotational echo. A clear enhancement in the signal intensities is seen for the *tert*-butyl methyl groups in the 1–10 μs region and 8–40 μs for the quaternary carbons. Furthermore, as shown by Munowitz and Griffin,[33] the rotational modulation can occur at integral multiples of the spinner period. This effect is evident near 200 μs ($1/\omega_r$) when the spinner rotated at *ca.* 5 kHz. From these results, speculation that for disulfide **1** the *tert*-butyl group is in a fast

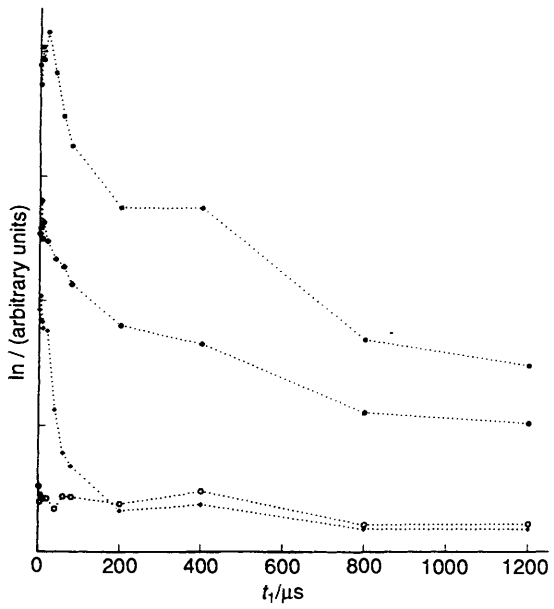

Fig. 11 Plot of ln*I versus* t_1 for the *tert*-butyl methyl groups (●, two upper traces), the quaternary carbon (○) and the methoxy group (◆) of the disulfide **3**

regime exchange whereas the phenyl group is static seems to be consistent with the X-ray data. The molecular packing displayed in Fig. 7 shows that the phenyl groups are in parallel planes ('sandwich'-type orientation) with a very limited degree of freedom. On the other hand, the *tert*-butyl groups have much more space for free rotation. In order to verify this hypothesis additional results were taken from one- and two-dimensional spin-diffusion experiments. The obtained results were found to be consistent with the first assumption. The absence of cross peaks in the two-dimensional plots when the mixing times were changed in the range 1–100 s further confirmed that the aromatic group does not undergo a dynamic process.[34]

The relationship between the intensities and the decay period t_1 in the dipolar-dephasing experiment for the disulfide **3** is shown in Fig. 11. As in the previous case, the decay of the intensity of the quaternary carbon was very slow. Spectacular results were obtained from the analysis of the decay of the methoxy groups. For a very short dephasing time, 1–60 μs, the methoxy signal decays very rapidly, for $t_1 > 100$ μs the signal decays very slowly. The data clearly show that the decay curve is biexponential and exhibits two significantly different time constants.

The dynamics in the solid of the methoxy group attached to the phosphorus is quite a complex phenomenon. We have shown[9] by employing broad-line ^{2}H NMR spectroscopy for perdeuteriated bis(dimethoxythiophosphoryl) disulfide that the methoxy groups rotate according to a three-fold jump model with reorientation of the methyl group about C_3 symmetry and an additional fast, small amplitude jump of the C_3 axis around the P–O bond.

These studies also revealed that the *tert*-butyl methyl groups in the disulfide **3** undergo fast reorientation in the solid. As in case of the disulfide **1** for a very short dephasing period, 1–10 μs, an enhancement of the signal intensities was observed. Moreover the rotational modulation is seen near 350 μs at the first spinner period ($\omega_r = 3$ kHz). From the decay-curve analysis of the *tert*-butyl methyl groups the biexponential character of the function is evident.

The preliminary low-temperature ^{13}C NMR studies for compound **1** showed a very low coalescence temperature for the methyl groups. The three separated signals for these groups are seen only at 138 K,[35] which is much lower than the temperatures recently reported by Riddell *et al.*[36] for the

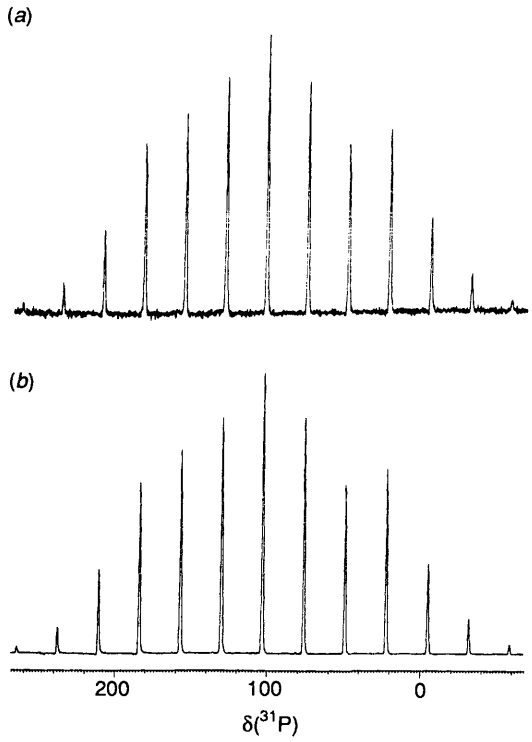

Fig. 12 Variable-temperature 121.49 MHz ^{31}P CP MAS NMR spectra for the disulfide **1** at (*a*) 363 and (*b*) 293 K

restricted rotation of the *tert*-butyl group of 1,1-dibenzyl-2,2-dimethylpropan-1-ol.

The tendency of the *tert*-butyl groups for fast molecular motion in the solid for model organic compounds has also been shown by Grant and co-workers[29] who employed the dipolar-dephasing experiment to reveal the rapid rotation of each methyl group and the *tert*-butyl group itself about its C_3 axis. Our results clearly show that the fast molecular motion of the *tert*-butyl group in the solid is not only limited to organic compounds but it is a common feature of phosphoroorganic moieties.

Since other dynamic processes can greatly perturb solid-state NMR spectra, in order to exclude the influence of rotation around the S–S and P–S bonds on the ^{13}C NMR resonances further results were obtained from variable-temperature ^{31}P CP MAS NMR experiments. Fig. 12 shows the ^{31}P CP MAS NMR spectra of the disulfide **1** at 293 and 363 K. The invariance of the anisotropy, asymmetry parameters and the resonance linewidth with temperature leads to the conclusion that the phosphorus nucleus is 'rigid' and the motion takes place only in the substituents. Similar results were also obtained for the disulfides **2** and **3**. The shielding parameters and principal elements of the chemical-shift tensors were calculated employing the graphical method of Herzfeld and Berger[37] from spinning sideband intensities. The solid-state ^{31}P NMR spectra for bis(organothiophosphoryl) disulfides are discussed in detail elsewhere.[38]

Conclusion

These studies show the power of the approach which employs X-ray crystallography and high-resolution solid-state NMR spectroscopy as complementary techniques in the elucidation of the structure and dynamics of organothiophosphoryl compounds.

The crystallographic results obtained are consistent with our previous hypothesis which suggested that S–S bond distances in the PSSP unit vary as a function of the torsional angle. Since disulfides with C–P–C, C–P–O and O–P–O bonds all obeyed this correlation it seems that the relationship discussed here is

general. The literature data for cyclic six-membered disulfides, where for PSSP angles of 72 and 86° the S–S distances were 2.06 and 2.03 Å respectively,[39,40] are in excellent agreement with the experimental curve in Fig. 4 and provide unambiguous evidence that this correlation is valid. The influence of the S–S–P=S conformation on the P–S bond length was also unambiguously assigned. Furthermore, our results for bis(organothiophosphoryl) disulfides show that the size of the substituents attached to the phosphorus have only a minute influence on the S–S bond conformation. This conclusion contradicts that of Jorgensen and Snyder[41] who showed that a CSSC skeleton steric congestion drives the bulkier disulfides in the direction of a *trans* geometry. Hence, it can be speculated that for the class of compounds under discussion the molecular-packing effect rather than the size of the substituents determines the conformation of the S–S bond, consistent with the data of Saenger and co-workers[42] who reported that a similar class of compounds with an O=PSSP=O backbone and bulky substituents are in the synclinal range.

The solid-state NMR results are consistent with monocrystal diffraction studies and provide useful information about the content and symmetry of the unit cell. The dipolar-dephasing experiments used as a tool for the investigation of the dynamic processes show that both the *tert*-butyl and methoxy groups are in a fast regime exchange. From variable-temperature ^{31}P CP MAS NMR experiments rotation around the disulfide S–S and P–S bonds were excluded.

Acknowledgements

The authors are grateful to Professor G. Grossmann (Technical University of Dresden, Germany) for access to X-ray diffraction data of bis(5,5-dimethyl-2-thiono-1,3,2λ^5-dioxaphosphorin-2-yl) disulfide prior to publication, to Mr. W. Ciesielski and Mr. S. Kaźmierski for technical assistance and to the Polish Academy of Sciences for financial support.

References

1 C. Fest and K. J. Schmidt, *The Chemistry of Organophosphorus Pesticides*, Springer, Berlin, New York, 2nd edn., 1982.
2 P. H. Molyneux, in *Lubrication and Lubricants*, ed. E. R. Braithwaite, Elsevier, Amsterdam, 1967, ch. 3.
3 M. Eto, *Organophosphorus, Pesticides, Organic and Biological Chemistry*, CRC Press, Cleveland, 1974.
4 P. G. Harrison, M. J. Begley, T. Kikabhai and F. Killer, *J. Chem. Soc., Dalton Trans.*, 1986, 925, 929; M. G. B. Drew, M. Hasan, R. J. Hobson and D. A. Rice, *J. Chem. Soc., Dalton Trans.*, 1986, 1161; J. A. McCleverty, R. S. Z. Kowalski, N. A. Bailey, R. Mulvaney and D. A. O'Clerigh, *J. Chem. Soc., Dalton Trans.*, 1983, 627; M. G. B. Drew, G. A. Forsyth, M. Hasan, R. J. Hobson and D. A. Rice, *J. Chem. Soc., Dalton Trans.*, 1987, 1027.
5 J. Michalski, A. Skowrońska and A. Łopusiński, *Phosphorus Sulfur*, 1991, **58**, 61 and refs. therein.
6 M. J. Potrzebowski, A. Łopusiński and J. Michalski, *Heteroat. Chem.*, 1991, **2**, 553.
7 P. J. Chu and M. J. Potrzebowski, *Magn. Reson. Chem.*, 1990, **28**, 477.
8 M. J. Potrzebowski, J. H. Reibenpies and Z. Zhong, *Heteroat. Chem.*, 1991, **2**, 455.
9 M. J. Potrzebowski, *Magn. Reson. Chem.*, 1992, **30**, 35.
10 A. Hordvik, *Acta Chem. Scand.*, 1966, **20**, 1885.
11 H. Sugeta, A. Go and T. Miyazawa, *Chem. Lett.*, 1972, 83.
12 H. E. Van Wart, A. Lewis, H. A. Scheraga and F. D. Saeva, *Proc. Natl. Acad. Sci. USA*, 1973, **70**, 2619.
13 H. E. Van Wart and H. A. Scheraga, *Proc. Natl. Acad. Sci. USA*, 1977, **74**, 13.
14 F. S. Jorgensen and J. P. Snyder, *J. Org. Chem.*, 1980, **45**, 1015.
15 W. Zhao, J. Bandeker and S. Krimm, *J. Am. Chem. Soc.*, 1988, **110**, 6891.
16 *Houben-Weyl Methoden der Organische Chemie*, XII/2, Georg Thieme, Stuttgart, 1964, p. 613; A. Łopusiński, L. Łuczak and J. Michalski, *J. Chem. Soc., Chem. Commun.*, 1989, 1694.
17 (*a*) B. A. Frenz, SDP Structure Determination Package, Enraf-Nonius, Delft, 1984; (*b*) A. C. T. North, D. C. Philips and F. S. Mathews, *Acta Crystallogr., Sect. A*, 1968, **24**, 351.
18 G. M. Sheldrick, G. M. Kruger and R. Goddard (Editors), SHELXS 86, *Crystallographic Computing 3*, Oxford University Press, 1985.
19 D. T. Gomer and J. T. Waber, *International Tables for X-Ray Crystallography*, Kynoch Press, Birmingham, 1974, vol. 4, pp. 55–59.
20 R. S. Cahn, C. K. Ingold and V. Prelog, *Angew. Chem., Int. Ed. Engl.*, 1966, **5**, 385.
21 A. Łopusiński, L. Łuczak, J. Michalski, A. E. Kozioł and M. Gdaniec, *J. Chem. Soc., Chem. Commun.*, 1991, 889.
22 S. Lawton, *Inorg. Chem.*, 1970, **9**, 2269.
23 G. Grossmann, personal communication.
24 M. Aida and C. Nagata, *Theor. Chim. Acta*, 1986, **70**, 73.
25 T. Burunda, A. C. Gallacher and A. A. Pinkerton, *Acta Crystallogr., Sect. C*, 1991, **47**, 1414.
26 C. A. Fyfe, *Solid State NMR for Chemists*, CFC Press, Guelph, Ontario, 1983; M. Mehring, *Principle of High Resolution NMR in Solids*, Springer, Berlin, 2nd edn., 1983.
27 C. E. Brown, *J. Am. Chem. Soc.*, 1982, **104**, 5608.
28 J. Witt, D. Fenzke and W.-D. Hoffmann, *Appl. Magn. Reson.*, 1992, **3**, 151.
29 L. B. Alemany, D. M. Grant, T. D. Alger and R. J. Pugmire, *J. Am. Chem. Soc.*, 1983, **105**, 6697.
30 M. Alla and E. Lippmaa, *Chem. Phys. Lett.*, 1976, **37**, 260.
31 D. E. Demco, J. Tegenfeldt and J. S. Waugh, *Phys. Rev. B*, 1975, **11**, 4133.
32 S. J. Opella and M. H. Frey, *J. Am. Chem. Soc.*, 1979, **101**, 5854.
33 M. G. Munowitz and R. G. Griffin, *J. Chem. Phys.*, 1982, **76**, 2848.
34 N. M. Szeverenyi, A. Bax and G. E. Maciel, *J. Am. Chem. Soc.*, 1983, **105**, 2579; N. M. Szeverenyi, M. J. Sullivan and G. E. Maciel, *J. Magn. Reson.*, 1982, **47**, 462.
35 G. Grossmann and M. J. Potrzebowski, unpublished work.
36 F. G. Riddell, S. Arumugan and J. E. Anderson, *J. Chem. Soc., Chem. Commun.*, 1991, 1525.
37 J. Herzfeld and A. B. Berger, *J. Chem. Phys.*, 1980, **73**, 1021.
38 M. J. Potrzebowski, *J. Chem. Soc., Perkin Trans. 2*, 1993, 63.
39 P. C. Minshall and G. M. Sheldrick, *Acta Crystallogr., Sect. B*, 1978, **34**, 1378.
40 F. W. B. Einstein, B. R. Penfold and Q. T. Tapsell, *Inorg. Chem.*, 1965, **4**, 186.
41 F. S. Jorgensen and J. P. Snyder, *Tetrahedron*, 1975, **35**, 1399.
42 C. H. Betzel, D. Loewus and W. Saenger, *Acta Crystallogr., Sect. C*, 1983, **39**, 270.

Received 11*th January* 1993; *Paper* 3/00170I